Solubilized Enzymatic Fuel Cell (SEFC) for Quasi-Continuous Operation Exploiting Carbohydrate Block Copolymer Glyconanoparticle Mediators

Jules Hammond, Andrew Gross, Fabien Giroud, Christophe Travelet, Redouane Borsali, Serge Cosnier

ACS Energy LETTERS

http://pubs.acs.org/journal/aelccp

Solubilized Enzymatic Fuel Cell (SEFC) for Quasi-Continuous Operation Exploiting Carbohydrate Block Copolymer Glyconanoparticle Mediators

Jules L. Hammond,[†] Andrew J. Gross,[†] Fabien Giroud,[†] Christophe Travelet,[‡] Redouane Borsali,*[,‡] and Serge Cosnier*[,†]

[†]Université Grenoble Alpes, CNRS, DCM, 38000 Grenoble, France

[‡]Université Grenoble Alpes, CNRS, CERMAV, 38000 Grenoble, France

Supporting Information

ABSTRACT: Enzymatic biofuel cells are ecofriendly power sources that can deliver μW−mW outputs from renewable substrates, but their stability is a major issue owing to enzyme fragility. The vast majority of reported biofuel cells can only generate power continuously for relatively short periods of time. Here we report a novel "solubilized enzymatic fuel cell (SEFC)" concept for continuous long-term operation. Avoiding surface immobilization techniques allows biocatalytic activity to be easily restored or replenished. The biofuel cell exploits freely diffusing enzymes and β-cyclodextrin-coated glyconanoparticles with entrapped quinone and thiazoline redox mediators, for mediated glucose and oxygen conversion. The cell was designed with permselective membranes to enable substrate and proton diffusion while trapping the enzymes and glyconanoparticles in separate compartments. The SEFC exhibited a peak power loss of only 26.3% after 7 days of continuous charge−discharge cycling at 50 μA; thus, SEFCs may be envisaged to power lab-on-a-chip devices for periods of several weeks.

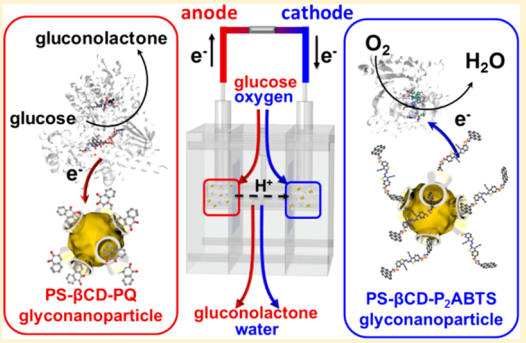

Enzymatic biofuel cells convert chemical energy into electrical energy by electroenzymatic reactions.[1] The use of enzymes provides several advantages compared to conventional noble metal catalysts, including very high specificity toward their substrates, high turnover and activity under mild conditions, and the ability to transform complex organic fuels. Enzymes are also biocompatible and environmentally benign, although intrinsically complex and fragile. Another major drawback of enzymes is their limited stability after immobilization on artificial electrode surfaces. Currently there is an urgent need to develop superior strategies to preserve, optimize, and enhance enzyme stability and activity at electrodes for bioelectrocatalysis under various conditions.

With state-of-the-art prototype biofuel cells already capable of powering small electronic devices such as pacemakers, lactate sensors, and wireless communication systems for short periods of time, their long-term operational stability remains a crucial parameter for their future success.[1−4] One of the key factors determining the lifetime of a biofuel cell is the stability of the enzymes and mediators, presenting pivotal concern for their practical application.[5] Immobilization of the enzyme on the electrode, for example, using carbon nanostructures,[6] often combined with surface modification chemistry, is considered to be the best way to stabilize the enzyme. However, this method eventually leads to a buildup of inactive enzyme at the surface, making it extremely difficult for the catalytic activity to be restored or replenished.[7] Enzyme immobilization and entrapment methods can also fix the enzymes in inefficient orientations, restricting their degrees of freedom and reducing their activity. Irreversible physical damage to the enzyme upon binding or cross-linking to the electrode is also an issue. Redox mediators are often immobilized together with the enzyme to facilitate electron shuttling to and from the enzyme's active site (mediated electron transfer (MET)). Covalent attachment of the enzyme followed by entrapment of the mediator by cross-linking,[8] encapsulation in polypyrrole films,[9] or forming a mixed compression with graphite particles[2] is typically used to stabilize enzymes at electrodes. Such techniques are considered to mitigate catalytic instability and minimize leaching[10] but at the expense of reduced activity. High concentrations of

Received: October 15, 2018
Accepted: December 3, 2018
Published: December 3, 2018

DOI: 10.1021/acsenergylett.8b01972
ACS Energy Lett. XXXX, XXX, XXX−XXX

immobilized mediators are typically required to maximize power density, but this can be difficult to realize, expensive, and unsafe due to toxicity, caused by progressive leaching.

The aim of this work is to depart from the traditional approach of immobilizing the bioelectrocatalytic components of the fuel cell on the electrodes. Instead, we adopt here a strategy of utilizing enzymes and redox-mediating glyconanoparticles (GNPs) solubilized (i.e., nonimmobilized) in solution. Enzymes and mediators in solution can freely diffuse and rotate for dynamic orientation with each other for effective electron transfer and bioelectrocatalysis. The use of enzymes in solution can also avoid issues related to poor mass transfer[11] and reproducibility due to complicated enzyme immobilization procedures.[12] Importantly, Zhu and Zhang[13] previously demonstrated that higher power densities can be obtained at a nonimmobilized bioanode of a closed biobattery when compared to an immobilized bioanode.

If both the enzymes and mediators are solubilized, as explored/reported herein, fresh biocatalysts can be introduced at high concentrations to restore or replenish performance by a simple exchange of the anode and cathode solutions. This will further prolong the biofuel cell lifetime and would address the major problem of conventional biofuel cells whereby the bioelectrodes with immobilized enzymes must be reconstructed when the enzyme becomes inactive. The concept of refueling the fuel solution of a biofuel cell has been previously demonstrated by Sony Corporation with an immobilized system. However, the cell voltage collapsed to 0.2 V after 40 fuel exchanges (200 min total operation).[14]

Taking into account that redox mediators and substrates such as glucose are similar in size, it was not possible to consider a solubilized bioelectrode system that was capable of retaining redox mediators while still permitting diffusion of glucose. In this context, the engineering of redox supramolecular entities exhibiting a similar size to proteins is a promising route in the design of bioelectrodes based on a size-exclusion process. GNP synthesis[15] not only allows hydrophobic and insoluble redox-active species to be solubilized but simultaneously enables size-dependent entrapment within a fuel cell compartment due to their large size via a size-exclusion membrane. Replacing classical redox mediators with redox-active GNPs opens up the new possibility to separate the anolyte from the catholyte and avoid cross-reaction. Without size exclusion there would be an inevitable drop in open-circuit voltage (OCV), close to zero, due to a mixed potential between the bioanode and biocathode. Furthermore, the use of GNPs can allow the redox-active anolyte/catholyte or fuel to be specifically replenished or restored.

In summary, we develop here the use of two types of freely diffusing, solubilized redox glycocopolymer nanoparticles for the electrical wiring of enzymes both at the anode and cathode. Furthermore, we have engineered a new solubilized enzymatic fuel cell (SEFC) device that integrates permselective membranes, allowing us to exploit the size of the GNPs to prevent mediator leaching into the fuel stream or away from their respective anode or cathode compartments.

The biofuel cell can be envisaged as the combination of two half-cells that concomitantly undergo oxidation and reduction reactions at the anode and cathode, respectively. Electrons produced by oxidation at the anode flow through the external circuit, delivering power to the load, and are then transferred to the cathode where they participate in the reduction reaction. As it is desirable to utilize abundant and low-cost organic energy sources, we base our system on glucose and oxygen as the fuel and oxidant, respectively. These substrates have attracted considerable attention for implantable and wearable applications, owing to their availability in the body in μM−mM concentrations by human metabolism and consumption, but are equally viable for portable applications.[1]

At the anode, we perform catalytic oxidation of glucose with fungal flavin adenine dinucleotide-dependent glucose dehydrogenase (FAD-GDH) from *Aspergillus sp.* using 9,10-phenanthrenequinone (PQ) as the organic redox mediator. PQ was recently shown to be an effective mediator in solution for glucose oxidation with this enzyme compared to other quinone mediators.[16] For the cathode, we reduce oxygen via a four-electron process to water using the bilirubin oxidase (BOx) enzyme from *Myrothecium verrucaria*, mediated by bispyrene-2,2′-azino-bis(3-ethylbenzothiazoline-6-sulfonic acid) (P_2ABTS).[15] In both cases, the mediator is encapsulated within a GNP using a guest−host interaction via β-cyclodextrin inclusion complexes. The two separate reactions occurring at the anode and cathode are illustrated in Figure 1.

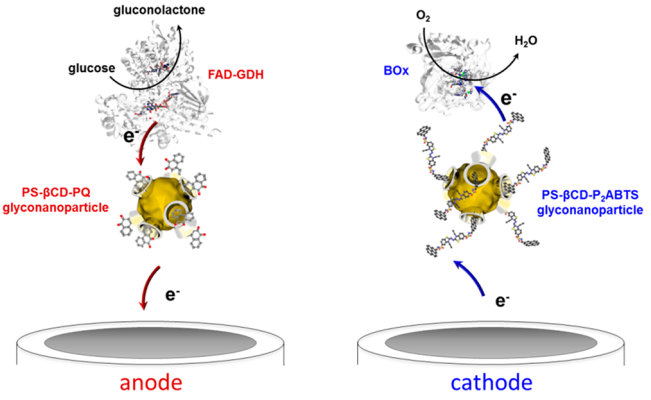

Figure 1. Scheme showing the reactions occurring at the anode (left) and cathode (right)

The redox GNPs were prepared using an amphiphilic β-cyclodextrin (β-CD) polystyrene diblock copolymer based on a click chemistry reaction. The β-CD GNPs are obtained by self-assembly with controlled encapsulation of the mediator in a high yield via the nanoprecipitation technique.[17] Further details of the P_2ABTS GNP preparation, characterization, and use for catalysis within a cathodic half-cell have been published previously by our group.[15] To complement the P_2ABTS GNPs and complete the aqueous biofuel cell, new GNPs with entrapped PQ as a redox mediator were developed for the anodic half-cell. We formed PS-βCD-PQ GNPs with approximate PQ concentrations of 34.2 and 68.4 μM (1:1 and 1:2, PS-βCD:PQ, mass). These concentrations are much higher than the maximum concentration achieved when dissolving PQ in deionized (DI) H_2O with ultrasonic agitation, of around 5 μM [SI, Figure S1]. This demonstrates how increased quantities of a hydrophobic mediator can be incorporated in solution for catalysis via host−guest encapsulation in our GNP system.

TEM imaging (Figure 2) of the PQ GNPs showed nanoparticles with average diameters of 20.0 ± 7.0 and 43.9 ± 27.7 nm at 34.2 and 68.4 μM, respectively. This compares to 43.3 ± 18.8 nm for the PS-βCD-P_2ABTS GNPs (SI, Figure S2). Interestingly, increasing the concentration of the guest altered the average GNP diameter, as shown in the size

DOI: 10.1021/acsenergylett.8b01972
ACS Energy Lett. XXXX, XXX, XXX−XXX

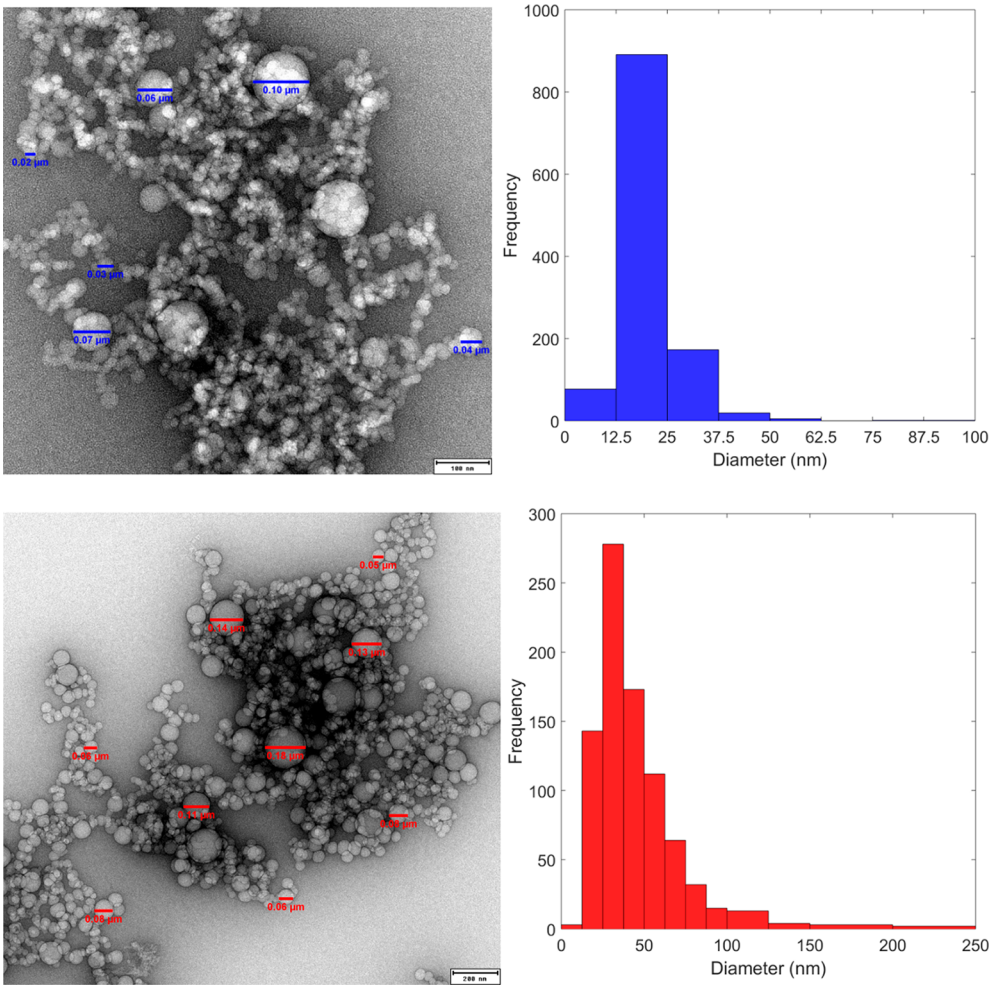

Figure 2. TEM images and histograms showing the typical size distribution of PS-βCD-PQ GNPs.

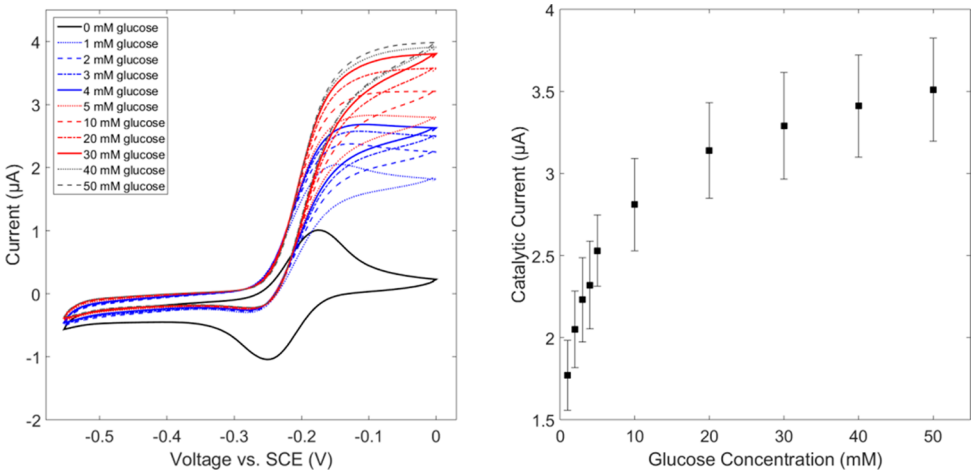

Figure 3. Cyclic voltammograms and glucose dose response for an anode half-cell using GCEs, 2.5 mL of 34.2 μM PS-βCD-PQ GNPs, and 0.3 mg of FAD-GDH in 25 μL of pH 7.0 McIlvaine buffer, ν = 5 mV·s^{-1}.

distributions (Figure 2), with this tendency also supported by the results of dynamic light scattering (DLS) experiments (SI, Figure S3 and Table S1). Importantly, the electroactivity of the PS-βCD-PQ GNPs is approximately doubled (1:1.91) when doubling the concentration of the mediator, as demonstrated by the scan-rate dependence shown on cyclic voltammograms (SI, Figures S4a,b and Table S2).

TEM images showed no change in the GNPs after 2 months or after addition of pH 7.0 McIlvaine buffer (data not shown). This is consistent with the apparent stability previously observed for our PS-βCD-P$_2$ABTS GNPs.[15] The electrocatalytic activity of the new PQ GNPs was then confirmed at glassy carbon electrodes (GCEs) with increasing concentrations of glucose in DI H_2O (Figure 3). Furthermore, system

DOI: 10.1021/acsenergylett.8b01972
ACS Energy Lett. XXXX, XXX, XXX−XXX

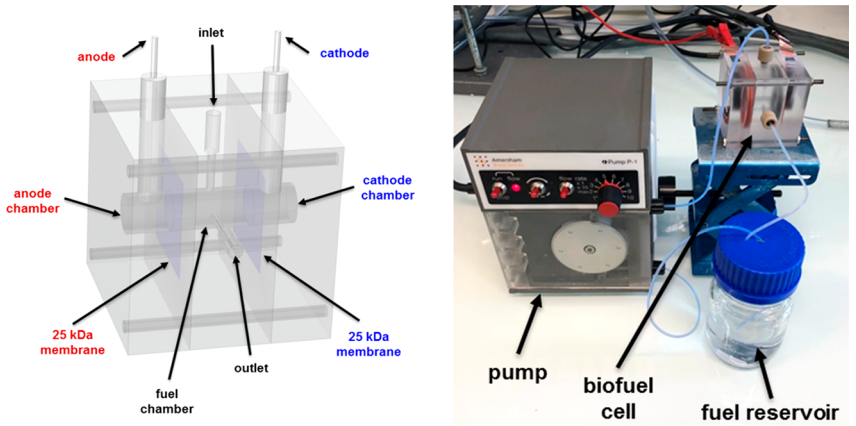

Figure 4. 3D annotated drawing (left) showing the fuel cell components and photograph (right) of the setup when connected.

performance was found to be limited by the enzyme mass (120 $\mu g \cdot mL^{-1}$) in the system (SI, Figure S5). At the higher bound of a typical blood glucose level (5 mM), the catalytic current was around 2.5 ± 0.2 μA.

f4 A new fuel cell (Figure 4) was developed specifically for our system and consists of three main parts. The central chamber (V = 1.5 mL) is connected to a peristaltic pump to provide a constant flow of fuel to the adjacent compartments (V = 1 mL) that contain the anode and cathode biocatalytic components. To prevent loss of the enzymes and mediators from their respective compartments, dialysis membranes with a cutoff value of 25 kDa are used as separators and sealed with a double O-ring system. This cutoff value translates to an approximate R_{min} of 1.9 nm (D_{min} = 3.9 nm), calculated using the following equation,[18] $R_{min} = 0.066(Da)^{1/3}$, and the cutoff value is sufficiently smaller than the diameter of PQ (20.0 ± 7.0 and 43.9 ± 27.7 nm at 34 and 68 μM, respectively) and P_2ABTS (43.3 nm ±18.8 nm) GNPs and the enzymes (BOx = 66−68 kDa and FAD-GDH = 95−135 kDa). Carbon nanotube buckypaper offers properties such as high specific surface area, mechanical flexibility, and high electrical conductivity.[19] To increase power output, electrodes with increased area (5 × 40 mm) were fabricated by attaching commercial carbon nanotube buckypaper to graphite foil current collectors using carbon paste. To limit evaporation and secure the electrodes in place, the compartments were sealed with tape and then the electrodes terminated with conductive adhesive copper tape.

A peristaltic pump operating at a flow rate of 80 $\mu L \cdot min^{-1}$ (mimicking typical blood vessel flow[20]) was used to deliver a continuous stream of pH 7.0 McIlvaine buffer containing ambient O_2 and 5 mM glucose from a 50 mL reservoir. A volume of 800 μL of PQ GNPs with 120 μg of FAD-GDH and 800 μL of P_2ABTS GNPs with 200 μg of BOx were injected into the anode and cathode compartments, respectively.

The electrocatalytic behavior of the bioelectrodes was verified for both half-cells (SI, Figures S6 and S7). Here we can compare the catalytic performance with our previous work on buckypaper electrodes[19] with immobilized enzyme and mediator bioelectrodes (see the SI for further details). Using a similar but not identical quinone mediator and FAD-GDH enzyme, we produced a catalytic output of 0.637 $mA.cm^{-2} \cdot mg^{-1}$. In contrast, the solubilized system with PQ GNPs and FAD-GDH reported here achieved 2.05 $mA \cdot cm^{-2} \cdot mg^{-1}$. Likewise, for the biocathode, prepared with immobilized BOx, we achieved 1.77 $mA \cdot cm^{-2} \cdot mg^{-1}$. This compares to a catalytic output of 3.79 $mA \cdot cm^{-2} \cdot mg^{-1}$ for the solubilized BOx system obtained in this work. We therefore clearly observe better catalytic performances per amount of enzyme catalyst in this work compared to state-of-the-art buckypaper anodes and cathodes with immobilized enzymes.

f5 Polarization plots (Figure 5) were performed for the biofuel cell by increasing the discharge current and recording the cell

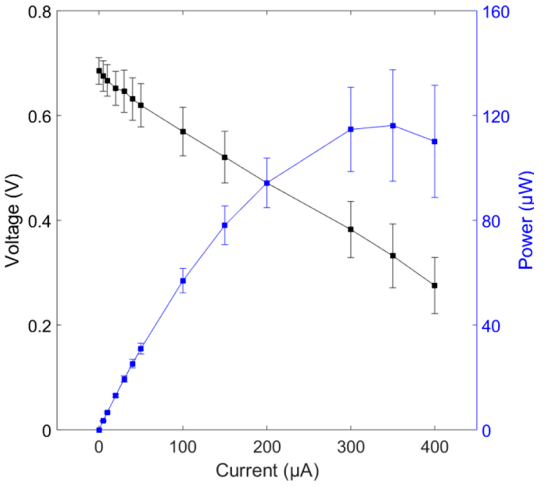

Figure 5. Cell performance (n = 3) showing voltage (black, left axis) and power (blue, right axis) as a function of current at a fuel flow rate of 80 $\mu L \cdot min^{-1}$ (pH 7.0 McIlvaine buffer with 5 mM glucose and ambient O_2), with 120 μg of FAD-GDH, 200 μg of BOx, and 800 μL of each GNP suspension.

voltage after 30 s. A maximum power point of 116.2 ± 21.3 μW was observed at a discharge current of 350 μA. The observed OCV of the fuel cell was 0.685 V ± 26 mV.

Operational stability of the fuel cell was tested by performing constant charge−discharge cycling for extended periods. The cell is discharged at a current of 50 μA until it reaches 0.25 V and then is allowed to recover until the voltage reaches 0.65 V. The glucose oxidation and oxygen reduction reactions are continuous. The selected current and voltage values provide a compromise between charge/discharge times, maximizing the duty cycle of power generation while also preventing damage to the enzyme. It is important to note that many previous reports of biofuel cell stability operate the device periodically for relatively short periods of time.

f6 A typical charge−discharge profile is shown in Figure 6a,b. The charge and discharge times were then calculated at

DOI: 10.1021/acsenergylett.8b01972
ACS Energy Lett. XXXX, XXX, XXX−XXX

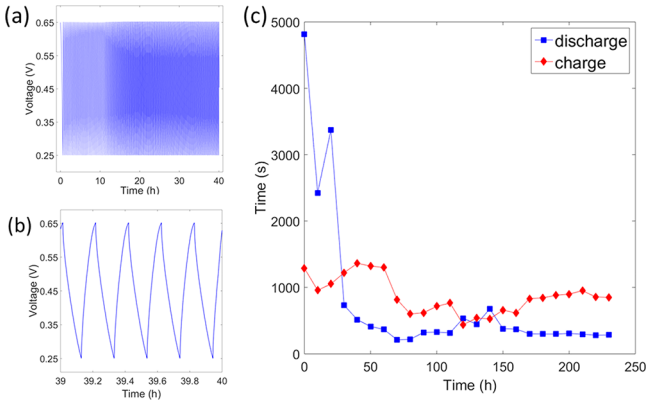

Figure 6. Typical charge−discharge cycles (a), zoomed period between 39 and 40 h (b), and plots of fuel cell discharge (blue, square marker) and charge (red, diamond marker) stability at 10 h intervals (c), all at a 50 μA discharge current and fuel flow rate of 80 μL·min^{-1} (pH 7.0 McIlvaine buffer with 5 mM glucose and ambient O_2) with 120 μg of FAD-GDH, 200 μg of BOx, and 800 μL of each GNP suspension.

intervals of 10 h and showed a stabilization of the discharge time after about 30 h (Figure 6c). After 10 days, the fuel cell still provided discharge times of around 5 min with charge times of around 15 min.

To provide a further indicator of the fuel cell stability, discharge tests at the peak discharge current (350 μA) were conducted at 2 and 7 days (typical discharge profiles shown in SI, Figure S8). This was to provide a further indicator for degradation of the fuel cell. After 2 days, the mean power was 115.3 ± 24.7 μW (n = 3), which is similar to the values obtained during initial characterization of the maximum power point during evaluation of the polarization profiles. At 7 days, the mean power dropped to 84.9 ± 2.9 μW (n = 5), equating to a power loss of 26.3%. As a comparison, a power loss of 65% was reported by Zhu and Zhang after operating the fuel cell for just 6 rounds of 2 h across a period of 12 days.

Furthermore, one fuel cell that was already subjected to 7 days of operational cycling at a discharge current of 50 μA was cycled at a higher discharge current of 350 μA for 24 h (SI, Figures S9−S11). This fuel cell provided relatively stable operational performance with discharge time falling from 20 to 15 s (−25%) and charge time increasing from 158 to 340 s (+115%). This demonstrates the ability to operate the biofuel cell at higher discharge currents over long periods of time while retaining a reasonable level of charge−discharge time stability.

The recirculating fuel solution was tested for the presence of any enzymes and mediators after completion of the operational stability tests and showed no evidence for catalysis (black lines), as shown by the control experiments (red/blue lines for anode/cathode, respectively; Figure 7a,b). This confirms that the biocatalytic elements are retained in their respective chambers and do not leach into the fuel stream. This is a testament to the GNPs, which, owing to their markedly larger sizes compared to classical redox mediators, provide the ability to constrain them within the anode and cathode compartments while allowing diffusion of the substrates, glucose, and oxygen. It is emphasized that redox mediators without nanoparticle encapsulation would not be retained owing to their smaller molecular size. A control experiment using classical redox mediators in place of the GNPs is described further below.

To check for the presence of adsorbed biocatalytic components, discharge profiles were performed following 7 days of operational cycling at 50 μA and after using different rinse techniques (SI, Figures S12 and S13). Although an OCV develops (after resting the cell for 2 h between each rinse), there is negligible power generated and no operational cycling can be performed, ruling out significant adsorption of the biocatalysts. The presence of only trace quantities of biocatalytic components is particularly attractive as the cell chambers can be effectively refreshed.

Finally, a control experiment without PS-βCD GNPs to encapsulate the mediators but instead with solubilized mediators was carried out. This control test confirmed that the addition of GNPs in the system helps to efficiently stabilize and improve performance. Without the GNPs, the performance was lower and rapidly degraded, with the charge times steadily increasing to the point that the cell failed to recharge after 20 h (SI, Figures S14 and S15). This was most likely

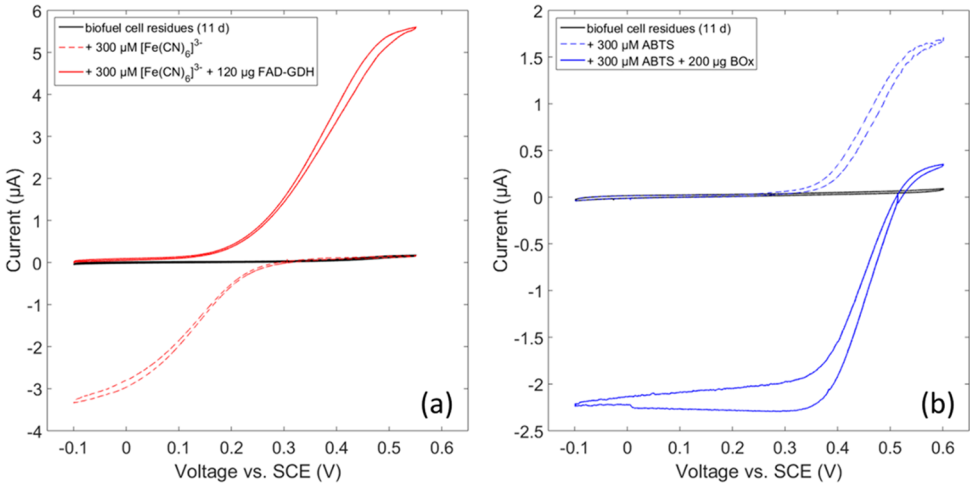

Figure 7. CVs showing response at GCEs for biofuel cell residues (black) with (a) +300 μM $[Fe(CN)_6]^{3-}$ (red, dashed) and +120 μg of FAD-GDH (red), all in saturated Ar with an Ar blanket, 2 mV·s^{-1}, and (b) +300 μM ABTS (blue, dashed) and +200 μg of BOx (blue), all in saturated O_2 with an O_2 blanket, 2 mV·s^{-1}.

DOI: 10.1021/acsenergylett.8b01972
ACS Energy Lett. XXXX, XXX, XXX−XXX

caused by the mediators readily leaching into the fuel flow and their concentration slowly diminishing.

To conclude, we demonstrated an enzymatic biofuel cell whereby the biocatalytic components are in the aqueous phase and therefore able to freely diffuse, shifting from the classical use of immobilized enzymes and mediators. With the use of GNPs made from the self-assembly of a carbohydrate-based block copolymer (β-cyclodextrin-*b*-PS), including new GNPs prepared with phenanthrenequinone, we show how increased quantities of mediator can be incorporated into the system to increase catalytic current. With the integration of carbon nanotube buckypaper electrodes into the diffusion-based biofuel cell, currents were enhanced by a factor of around 85, relative to GCEs. We have also shown that this novel fuel cell design significantly extends the operational lifetime, for example, by preventing leaching of the mediator through a permselective membrane. After 7 days of operation, the peak power of the optimized biofuel cell only dropped by 26% to 84.9 μW. Further, we clearly show evidence that the use of enzymes in solution can be a viable approach in biofuel cell design, contrary to the general consensus in the literature. A further advantage of this diffusion-based biofuel cell, to be explored in the future, is the possibility to easily recycle and refresh the biocatalytic components. It is feasible that SEFCs, alongside a boost converter, could be used as a green power source for powering low-power portable lab-on-a-chip electronics to perform functions such as quasi-continuous monitoring with data transmission.

■ ASSOCIATED CONTENT

Supporting Information

The Supporting Information is available free of charge on the ACS Publications website at DOI: 10.1021/acsenergylett.8b01972.

Full details of reagents, materials, and experimental methods, further optical, electrochemical, and electronic characterization, results from control tests, as well as calculations comparing systems with immobilized versus solubilized biocatalysts (PDF)

■ AUTHOR INFORMATION

Corresponding Authors

*E-mail: redouane.borsali@univ-grenoble-alpes.fr (R.B.).
*E-mail: serge.cosnier@univ-grenoble-alpes.fr (S.C.).

ORCID

Jules L. Hammond: 0000-0002-3308-5421
Andrew J. Gross: 0000-0002-7356-7089
Fabien Giroud: 0000-0001-6611-2687

Notes

The authors declare no competing financial interest.

■ ACKNOWLEDGMENTS

We gratefully acknowledge the financial support of LabEx ARCANE (ANR-11LABX-0003-01) and the Institut Carnot PolyNat (CARN 0007-01) for postdoctoral funding. We also acknowledge the support of the ICMG Chemistry Nanobio Platform for providing facilities (PCN-ICMG).

■ REFERENCES

(1) Cosnier, S.; Gross, A. J.; Le Goff, A.; Holzinger, M. Recent Advances on Enzymatic Glucose/Oxygen and Hydrogen/Oxygen Biofuel Cells: Achievements and Limitations. *J. Power Sources* **2016**, *325*, 252−263.

(2) Cinquin, P.; Gondran, C.; Giroud, F.; Mazabrard, S.; Pellissier, A.; Boucher, F.; Alcaraz, J.-P.; Gorgy, K.; Lenouvel, F.; Mathé, S.; et al. A Glucose BioFuel Cell Implanted in Rats. *PLoS One* **2010**, *5* (5), No. e10476.

(3) MacVittie, K.; Halamek, J.; Halámková, L.; Southcott, M.; Jemison, W. D.; Lobel, R.; Katz, E. From "Cyborg" Lobsters to a Pacemaker Powered by Implantable Biofuel Cells. *Energy Environ. Sci.* **2013**, *6*, 81−86.

(4) Monsalve, K.; Mazurenko, I.; Lalaoui, N.; Le Goff, A.; Holzinger, M.; Infossi, P.; Nitsche, S.; Lojou, J. Y.; Giudici-Orticoni, M. T.; Cosnier, S.; et al. A H_2/O_2 Enzymatic Fuel Cell as a Sustainable Power for a Wireless Device. *Electrochem. Commun.* **2015**, *60*, 216−220.

(5) Moehlenbrock, M. J.; Minteer, S. D. Extended Lifetime Biofuel Cells. *Chem. Soc. Rev.* **2008**, *37* (6), 1188.

(6) Mazurenko, I.; Monsalve, K.; Infossi, P.; Giudici-Orticoni, M.-T.; Topin, F.; Mano, N.; Lojou, E. Impact of Substrate Diffusion and Enzyme Distribution in 3D-Porous Electrodes: A Combined Electrochemical and Modelling Study of a Thermostable H_2/O_2 Enzymatic Fuel Cell. *Energy Environ. Sci.* **2017**, *10* (9), 1966−1982.

(7) Rubenwolf, S.; Kerzenmacher, S.; Zengerle, R.; von Stetten, F. Strategies to Extend the Lifetime of Bioelectrochemical Enzyme Electrodes for Biosensing and Biofuel Cell Applications. *Appl. Microbiol. Biotechnol.* **2011**, *89* (5), 1315−1322.

(8) Merle, G.; Habrioux, A.; Servat, K.; Rolland, M.; Innocent, C.; Kokoh, K. B.; Tingry, S. Long-Term Activity of Covalent Grafted Biocatalysts during Intermittent Use of a Glucose/O_2 Biofuel Cell. *Electrochim. Acta* **2009**, *54* (11), 2998−3003.

(9) Kim, J.; Kim, S. I.; Yoo, K.-H. Polypyrrole Nanowire-Based Enzymatic Biofuel Cells. *Biosens. Bioelectron.* **2009**, *25* (2), 350−355.

(10) Schuhmann, W.; Wohlschläger, H.; Lammert, R.; Schmidt, H. L.; Löffler, U.; Wiemhöfer, H. D.; Göpel, W. Leaching of Dimethylferrocene, a Redox Mediator in Amperometric Enzyme Electrodes. *Sens. Actuators, B* **1990**, *1* (1−6), 571−575.

(11) Johnston, W.; Maynard, N.; Liaw, B. Y.; Cooney, M. J. In Situ Measurement of Activity and Mass Transfer Effects in Enzyme Immobilized Electrodes. *Enzyme Microb. Technol.* **2006**, *39* (1), 131−140.

(12) Zhao, X.; Jia, H.; Kim, J.; Wang, P. Kinetic Limitations of a Bioelectrochemical Electrode Using Carbon Nanotube-Attached Glucose Oxidase for Biofuel Cells. *Biotechnol. Bioeng.* **2009**, *104* (6), 1068−1074.

(13) Zhu, Z.; Zhang, Y.-H. P. Use of Nonimmobilized Enzymes and Mediators Achieved High Power Densities in Closed Biobatteries. *Energy Sci. Eng.* **2015**, *3* (5), 490−497.

(14) Fujita, S.; Yamanoi, S.; Murata, K.; Mita, H.; Samukawa, T.; Nakagawa, T.; Sakai, H.; Tokita, Y. A Repeatedly Refuelable Mediated Biofuel Cell Based on a Hierarchical Porous Carbon Electrode. *Sci. Rep.* **2015**, *4* (1), 4937.

(15) Gross, A. J.; Chen, X.; Giroud, F.; Travelet, C.; Borsali, R.; Cosnier, S. Redox-Active Glyconanoparticles as Electron Shuttles for Mediated Electron Transfer with Bilirubin Oxidase in Solution. *J. Am. Chem. Soc.* **2017**, *139* (45), 16076−16079.

(16) Tsuruoka, N.; Sadakane, T.; Hayashi, R.; Tsujimura, S. Bimolecular Rate Constants for FAD-Dependent Glucose Dehydrogenase from *Aspergillus Terreus* and Organic Electron Acceptors. *Int. J. Mol. Sci.* **2017**, *18* (3), 604.

(17) Gross, A. J.; Haddad, R.; Travelet, C.; Reynaud, E.; Audebert, P.; Borsali, R.; Cosnier, S. Redox-Active Carbohydrate-Coated Nanoparticles: Self-Assembly of a Cyclodextrin−Polystyrene Glycopolymer with Tetrazine−Naphthalimide. *Langmuir* **2016**, *32* (45), 11939−11945.

(18) Erickson, H. P. Size and Shape of Protein Molecules at the Nanometer Level Determined by Sedimentation, Gel Filtration, and Electron Microscopy. *Biol. Proced. Online* **2009**, *11* (1), 32−51.

(19) Gross, A. J.; Chen, X.; Giroud, F.; Abreu, C.; Le Goff, A.; Holzinger, M.; Cosnier, S. A High Power Buckypaper Biofuel Cell:

DOI: 10.1021/acsenergylett.8b01972
ACS Energy Lett. XXXX, XXX, XXX−XXX

440 Exploiting 1,10-Phenanthroline-5,6-Dione with FAD-Dependent
441 Dehydrogenase for Catalytically-Powerful Glucose Oxidation. *ACS*
442 *Catal.* **2017**, *7* (7), 4408−4416.
443 (20) Wang, Y.; Lu, A.; Gil-Flamer, J.; Tan, O.; Izatt, J. A.; Huang, D.
444 Measurement of Total Blood Flow in the Normal Human Retina
445 Using Doppler Fourier-Domain Optical Coherence Tomography. *Br.*
446 *J. Ophthalmol.* **2009**, *93* (5), 634−637.

DOI: 10.1021/acsenergylett.8b01972
ACS Energy Lett. XXXX, XXX, XXX−XXX